DALTON

Studies of octameric vinylsilasesquioxane by carbon-13 and silicon-29 cross polarization magic angle spinning and inversion recovery cross polarization nuclear magnetic resonance spectroscopy

Christian Bonhomme,*[a] Paul Tolédano,[a] Jocelyne Maquet,[a] Jacques Livage[a] and Laure Bonhomme-Coury†[b]

[a] *Laboratoire Chimie de la Matière Condensée, Université Paris 6, 4 Place Jussieu, 75252 Paris Cedex 05, France*
[b] *Laboratoire Céramiques et Matériaux Minéraux, Ecole Supérieure de Physique et Chimie Industrielles de la Ville de Paris, 10 rue Vauquelin, 75231 Paris Cedex 05, France*

The acidic hydrolysis of triethoxyvinylsilane $Si(C_2H_3)(OEt)_3$ led to octavinyloctasilasesquioxane $(C_2H_3SiO_{1.5})_8$ **1** and to a transparent derived gel **2**. Compound **1** was obtained as single crystals, suitable for X-ray analysis: trigonal, space group $R\bar{3}$, $Z = 3$, $a = 13.533(2)$, $c = 14.222(2)$ Å, $\gamma = 120°$. Disorder of the methylene groups was observed. Compound **1** was carefully studied by IR spectroscopy and $^{29}Si/^{13}C$ cross polarization magic angle spinning (CP MAS) NMR spectroscopy. The CP dynamics of the various ^{13}C sites were analysed by inversion recovery cross polarization (IRCP). Very different behaviours were observed for CH and CH_2 signals and could be attributed to anisotropic reorientations of the vinyl groups. The IRCP sequence enabled a complete editing of the spectra and definite assignments of the observed lines. Owing to its highly resolved spectra and small intrinsic linewidths, it appears that compound **1** could act as a secondary reference for the set-up of the Hartmann–Hahn condition in ^{29}Si CP NMR spectroscopy as well as a test for the set-up of the magic angle. All these results were applied to the study of the amorphous gel **2**. Dipolar coupling constants were also strongly affected by local motions.

During the last few years, spherosiloxanes, including octameric silasesquioxanes $(RSiO_{1.5})_8$, have been extensively studied. Several review articles have been published.[1–4] Special attention was paid to syntheses of new silasesquioxane structures[5,6] including heterometallic silasesquioxanes.[2,7,8] This class of compounds has been used as models in different fields such as silicate/zeolite chemistry, catalytic and analytical chemistry, *etc*. Therefore, silasesquioxanes have been studied by different spectroscopic techniques, *i.e.* X-ray diffraction,[9–16] neutron diffraction,[17] vibrational spectroscopies[14,18] including normal coordinate analysis, liquid-state (^1H, ^{29}Si, ^{13}C and ^{17}O) NMR,[6,19,20] *etc.* A few crystalline silasesquioxanes were studied by ^{29}Si and ^{13}C solid-state NMR spectroscopy, including the 'Q_8M_8' derivative $(Me_3SiOSiO_{1.5})_8$, which is now widely used for the set-up of ^{29}Si cross polarization magic angle spinning (CP MAS) NMR.[21,22] Moreover, interest in the use of these compounds as precursors for ceramics and macromolecular materials, by bridging organofunctional silasesquioxanes, has grown significantly very recently.[4,23–25]

Vinyl derivatives and heterofunctional compounds have been widely investigated by Martynova and co-workers[26,27] including X-ray diffraction studies.[10] In this paper we present a complete study of the 'cubane shaped' octavinyloctasilasesquioxane $(C_2H_3SiO_{1.5})_8$ **1** by X-ray diffraction, infrared and $^{29}Si/^{31}C$ solid-state CP MAS NMR spectroscopy; ^{29}Si CP MAS NMR spectroscopy was used to extract isotropic chemical shifts as well as chemical shift anisotropies (CSAs). Few CSA values related to small organosilicon molecules are available in the literature. Such CSAs may give information on the electronic environment around ^{29}Si nuclei, local structure and molecular motion if present. The CP MAS NMR technique was not only used for enhancing the nuclear spin magnetization,[28] but was also successfully used to edit the spectra, *i.e.* to assign without ambiguity the observed ^{13}C resonances. The inversion recovery cross polarization (IRCP) sequence can be compared to the well known editing sequences in liquid-state NMR, *e.g.* distortionless enhancements by polarization transfer (DEPT) and insensitive nuclei enhanced by polarization transfer (INEPT).[29] Such editing techniques could act as invaluable tools of investigation for bridged-silasesquioxane amorphous materials. Indeed, the determination of the proton multiplicities of ^{13}C sites is crucial for the complete characterization of these compounds. Moreover, the study of the CP dynamics allowed us to investigate local motion of the vinyl groups and to propose simple geometrical explanations for the astonishing CP behaviour of adjacent CH and CH_2 groups. The results were applied to the study of an amorphous gel (compound **2**) containing mostly vinyl T^3 units(*), *i.e.* fully condensed $C_2H_3Si^*(OSi\equiv)_3$ entities.

† E-Mail: laure.bonhomme@espci.fr

Results and Discussion

Syntheses

Synthesis of $(C_2H_3SiO_{1.5})_8$ **1** and the derived gel **2** are described in the Experimental section. Hydrolysis under acidic conditions and subsequent condensation of an organically modified silicon alkoxide, triethoxyvinylsilane $Si(C_2H_3)(OEt)_3$ led to: (*i*) crystals (compound **1**) with only fully condensed T^3 units and (*ii*) gels (compound **2**) containing *a priori* $T^{0–3}$ units(*), $C_2H_3Si^*X_{3-x}(OSi\equiv)_x$ (X = OH or OEt, $x = 0–3$).

Hydrolytic polycondensation of organotrichloro- (or methoxy-) silanes seems to be the main route of synthesis: Martynova and Chupakhina[27] obtained octaorganooctasilasesquioxanes containing both methyl and vinyl groups by hydrolysis of $SiMeCl_3$ and $Si(C_2H_3)Cl_3$; Hendan and Marsmann[19] presented the synthesis of mixed ethyl and vinyl derivatives starting from $SiEtCl_3$ and $Si(C_2H_3)Cl_3$.

The use of modified silicon alkoxides $SiR(OR')_3$ (R = H or organic group, R′ = organic group) may open new synthetic routes to hydrido- and/or organo-silasesquioxanes. In particular,

Table 1 Selected bond lengths (Å) and angles (°) with estimated standard deviations in parentheses for $C_{16}H_{24}Si_8O_{12}$ **1**. Symmetry codes as in Fig. 1

Si(1)–O(1)	1.606(6)	C(1)–C(11)	1.25(3)
Si(2)–O(1)	1.596(6)	C(2)–C(21)	1.22(3)
Si(2)–O(2)	1.596(6)	C(2)–C(22)	1.26(3)
Si(2)–O(2^{V})	1.616(6)	C(2)–C(23)	1.23(4)
Si(1)–C(1)	1.81(2)	C(2)–C(24)	1.27(4)
Si(2)–C(2)	1.82(1)		
O(1)–Si(1)–O(1^{II})	108.5(3)	Si(1)–O(1)–Si(2)	150.5(4)
O(1)–Si(2)–O(2)	108.5(3)	Si(2)–O(2)–Si(2^{IV})	150.0(4)
O(1)–Si(2)–O(2^{V})	108.7(4)	Si(1)–C(1)–C(11)	127(2)
O(2)–Si(2)–O(2^{V})	108.6(3)	Si(2)–C(2)–C(21)	128(2)
O(1)–Si(1)–C(1)	110.5(3)	Si(2)–C(2)–C(22)	121(2)
O(1)–Si(2)–C(2)	110.0(5)	Si(2)–C(2)–C(23)	132(3)
O(2)–Si(2)–C(2)	111.4(5)	Si(2)–C(2)–C(24)	125(3)
O(2^{V})–Si(2)–C(2)	109.7(5)		

the choice of the experimental parameters (pH, temperature, solvent, concentration, nature of R′) allows a partial control of the hydrolysis–condensation process.[30] Hydrolysis of such alkoxides leads to polymeric gels, which can act as ceramic precursors.[4] In this context, the formation of crystalline phases (such as compound **1**) from media which usually lead to amorphous gels is a very interesting starting point for spectroscopic studies of such gels. This could be especially valuable for NMR studies of amorphous or poorly crystallized materials, which are extensively investigated by $^{13}C/^{29}Si/^{1}H$ solid-state NMR techniques.[31,32] In the case of compound **1** one unique crystalline phase is obtained, in contrast with the synthesis proposed by Baidina *et al.*[10] [*i.e.* direct hydrolysis of $Si(C_2H_3)Cl_3$] leading to octa- and deca-silasesquioxanes $(C_2H_3SiO_{1.5})_n$ with $n = 8$ or 10. However, in our case, the reaction yield for compound **1** remains poor.

Crystal structure of compound 1

The molecular structure of compound **1**, $C_{16}H_{24}Si_8O_{12}$, is shown in Fig. 1. Only the second vinyl carbons C(11) and C(21) are represented as the structure is disordered (see below). Selected bond lengths and angles are presented in Table 1. The main feature of the octameric cluster is the presence of a C_3 axis containing atoms C(1) and Si(1). Disorder at the CH_2 sites is present. Atom C(11) is bonded to C(1) (located on the C_3 axis). Four positions for carbon atoms bonded to C(2) were found, corresponding to C(21)–C(24). Fractional occupancies of C(11) and C(21)–C(24) were refined for the structure solution. The occupancy of C(11) was found to be $\frac{1}{3}$. Such a characteristic has been previously clearly evidenced by Larsson,[9] in the case of isomorphous homologues belonging to the hexagonal system and showing space group $R\bar{3}$ [*e.g.* $(RSiO_{1.5})_8$, R = Me, Et, Pr^n and Pr^i]. This has been also observed by Baidina *et al.*[10] in the case of the octavinyl derivative (trigonal, space group $R\bar{3}$, $a = 13.584$, $c = 14.364$ Å, final $R = 0.11$). However, several differences between the molecular structure of the octavinyl derivative described in ref. 10 and compound **1** have to be noted. First, the Si–C bond lengths are shorter in our work than in ref. 10 to a rather important extent: Si(1)–C(1) and Si(2)–C(2) 2.03 Å in ref. 10, whereas we found 1.81(2) and 1.82(1) Å, respectively. Secondly, two distinct positions (with site occupancy $\approx \frac{1}{2}$) seem to be sufficient to describe the methylene carbon atom in the general position in ref. 10, whereas, in the case of compound **1** four disordered methylene positions C(21)–C(24) were found with site occupancies varying from 0.15 to 0.39 as estimations.

The Si–O and Si–C bond lengths as well as O–Si–O, Si–O–Si and O–Si–C angles are in accord with values observed for well characterized octameric silasesquioxanes.[11,12,14] The Si(2)–C(2)–C angles have a mean value of 127(3)°, in agreement with the Si(1)–C(1)–C(11) angle [127(2)°]. All C=C bond lengths are close to 1.25 Å (significantly shorter than usual, *i.e.* 1.33 Å). These observations justify the fact that positions C(21)–C(24) correspond to methylene sites but they are surely estimations. One unique C(21) position (occupancy = 1) cannot be defined.

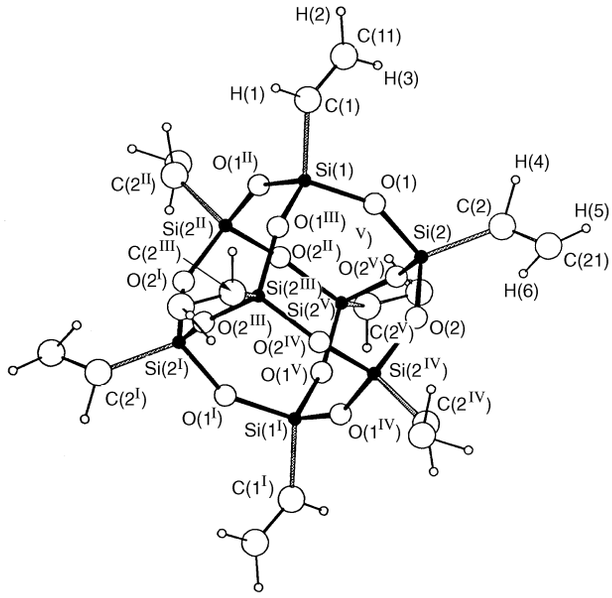

Fig. 1 An ORTEP[33] view of the structure of $C_{16}H_{24}Si_8O_{12}$ **1**, showing the atom labelling scheme. Of the second vinyl carbons only C(11) and C(21) are represented as well as their bonded hydrogens (calculated positions). The CH_2 positions are disordered (see text). Symmetry codes: I $\bar{x}, \bar{y}, \bar{z}$; II $\bar{y}, x-y, z$; III $y-x, \bar{x}, z$; IV $y, y-x, \bar{z}$; V $x-y, x, \bar{z}$

There are two non-equivalent distances between centrosymmetrically related silicon atoms within the molecule. Opposite Si atoms in general positions are 5.371(5) Å apart and those on the C_3 axis are 5.360(1) Å apart. Such a slightly distorted cubane structure is accompanied by the absence of Si–O intermolecular contacts less than 3.7 Å and a low crystal density ($D_c = 1.398$ g cm^{-3}). An increase in the number of short intermolecular Si–O contacts led to more important distortions of the cubane cores as well as to an increase in crystal density.[14] Larsson[9] showed also that the crystal density decreased from 1.51 g cm^{-3} for $(MeSiO_{1.5})_8$ to 1.09 g cm^{-3} in $(Pr^nSiO_{1.5})_8$.

The main characteristic of compound **1** is the non-equivalence of the vinyl groups. The C(11) positions are related by C_3 symmetry, whereas C(21)–C(24) are non-symmetry-related. As X-ray diffraction is unable to distinguish between static and dynamic disorder the vinyl groups are either disordered or in motion.

Vibrational spectroscopy

Compounds **1** and **2** were analysed by infrared spectroscopy. Assignments of the main bands are given in Table 2, based on data from the literature.[14,31,34] The IR spectrum of neat $Si(C_2H_3)(OEt)_3$ was also used as a reference.

The IR spectrum of compound **1** is characterized by a very strong band centred at 1113 cm^{-1}, assigned to ν_{asym}(Si–O–Si). This band is broad, compared to the other vibrations ($\Delta w_{\frac{1}{2}} \approx 100$ cm^{-1}). It is interesting that the other bands assigned to specific vibrations of the cubic siloxane cage ($\nu \leqslant 780$ cm^{-1}) are also rather broad, when compared to bands involving only the organic part of the molecule. This may reflect the small distortions of the cubane cage, lowering the symmetry of the entity from O_h. The band centred at 780 cm^{-1} has a shoulder (756 cm^{-1}) which could indicate the presence of two Si–C bonding types, as already seen by X-ray analysis.

Table 2 Selected infrared absorptions (cm^{-1}) of $C_{16}H_{24}Si_8O_{12}$ **1** and the gel **2**

1	**2**	Assignment*
3067w	3063w	$\nu_{asym}(CH_2)$
3026w	3024w	$\nu(CH)$
1604m	1603m	$\nu(C{=}C)$
1409m	1409m	$\delta(CH_2)$ in plane
1277m	1278m	$\delta(CH)$ in plane
1152 (sh)		
1113vs (br)	1129vs (br)	$\nu_{asym}(Si{-}O{-}Si)$
	1043s (br)	
1005m	1005m	$\delta(CH)$ out of plane
970m	963m	$\delta(CH_2)$ out of plane
780m	762m (br)	$\nu(Si{-}C)$
756 (sh)		
585s	587m (br)	$\delta(O{-}Si{-}O)$
	546m	$+\delta(Si{-}C{=}C)$
465w	428m (br)	$\nu_{sym}(Si{-}O{-}Si)$

* According to refs. 14, 31 and 34. w = Weak, m = medium, s = strong, br = broad, sh = shoulder, v = very, sym = symmetric, asym = asymmetric.

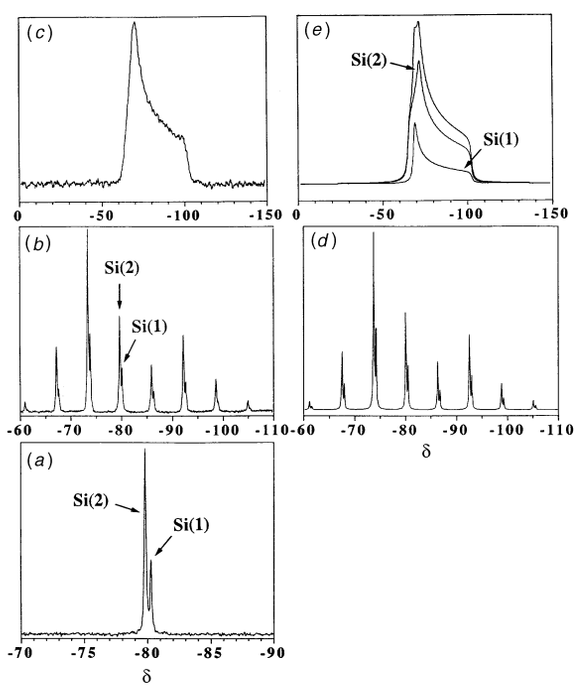

Fig. 2 The ^{29}Si CP MAS NMR spectra of compound **1**: (*a*) 'high' rotation speed, ν_{rot} (rotation speed) = 4000 Hz, Ξ (^{29}Si) (Larmor frequency) = 59.62 MHz, φ (diameter of rotor) = 4 mm, N_s (number of scans) = 8, t_{CP} (contact time) = 10 ms, r.d. (recycle delay) = 15 s, l.b. (line broadening) = 0 Hz; (*b*) 'intermediate' rotation speed, ν_{rot} = 500 Hz, Ξ (^{29}Si) = 79.50 MHz, φ = 7 mm, N_s = 200, t_{CP} = 10 ms, r.d. = 15 s, l.b. = 3 Hz, isotropic resonances labelled by arrows [(*d*) simulation of sideband patterns]; (*c*) static experiment, ν_{rot} = 0 Hz, Ξ (^{29}Si) = 59.62 MHz, φ = 7 mm, N_s = 400, t_{CP} = 10 ms, r.d. = 15 s, l.b. = 20 Hz [(*e*) simulations of Si(1) and Si(2) powder patterns convoluted by a gaussian broadening]

The IR spectrum of the xerogel **2** is very similar to that for **1**. All the bands (ν < 2000 cm^{-1}) already assigned to vinyl vibrations for **1** are observed as five sharp signals centred at 1603, 1409, 1278, 1005 and 963 cm^{-1}. However, bands involving Si–O and Si–C vibrations are broadened, leading to a less resolved spectrum at low frequency. Such a broadening can be safely related to more disordered and/or distorted environments around Si atoms (compound **2** is amorphous to X-rays). Vibrations related to vinyl groups are much less sensitive to this disorder. Although not quantitative, this spectrum suggests that the xerogel contains very few residual ethoxy groups: no clear vibration is observed in the range 1350–1500 cm^{-1} (relative to aliphatic CH_2 and CH_3 deformations). This gel is highly condensed (*i.e.* it contains mainly T^3 units) as has been shown by solid-state ^{13}C NMR spectroscopy (see below).

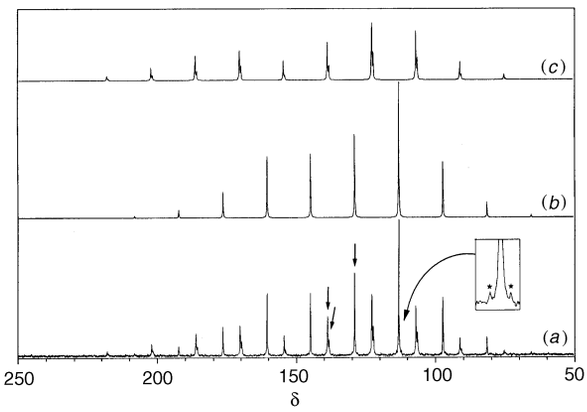

Fig. 3 The ^{13}C CP MAS NMR spectrum of compound **1** (*a*), with simulations of CH (*b*) and CH_2 (*c*) patterns. Isotropic resonances are labelled by arrows: ν_{rot} = 1200 Hz, Ξ (^{13}C) = 75.46 MHz, φ = 7 mm, N_s = 104, t_{CP} = 5 ms, r.d. = 15 s, l.b. = 3 Hz. * Satellites corresponding to $^1J(^{13}C{-}^{29}Si)$

Solid-state NMR spectroscopy

Compound 1. *Standard* ^{29}Si *and* ^{13}C *CP MAS experiments.* Spectra of compound **1** obtained by ^{29}Si and ^{13}C CP MAS experiments (at various rotation speeds) are presented in Figs. 2 and 3, respectively. All NMR data, including isotropic chemical shift (^{29}Si and ^{13}C), shielding tensor principal components, linewidths, relative intensities and assignments are presented in Table 3.

Few data concerning solid-state ^{29}Si NMR results for silasesquioxanes are available. Most of the ^{29}Si chemical shift data were obtained in solution including sophisticated two-dimensional experiments [*i.e.* incredible natural abundance double quantum transfer experiment (INADEQUATE)[19]] and leading to correlations between chemical shifts and geometrical parameters.[6] Hoebbel and co-workers[22,35,36] studied several octa- and decasilasesquioxanes by means of solid-state techniques but published only isotropic chemical shift values. The determination of the principal components of the tensor σ (chemical shift tensor) was mainly devoted to the structure elucidation of silicate minerals.[37] To our knowledge, few papers dealing with shielding tensors of molecular organosilicon compounds have been published so far. Harris *et al.*[38] presented ^{29}Si NMR studies of various polysilanes, exhibiting different silicon environments.

Compound **1** is characterized by two isotropic ^{29}Si peaks [Fig. 2(*a*) and Table 3] characteristic of T^3 units. The intensities of the lines are in the ratio 3:1 in good agreement with the presence of three equivalent Si(2) atoms to one Si(1) located on the C_3 axis. This allows definite assignments for both resonances. It should be noted that a small shielding of Si atoms located on the C_3 axis was also observed in the case of the octamethyl cubane derivative $(MeSiO_{1.5})_8$:[22] $\delta_{Si(1)}$ −66.5 and $\delta_{Si(2)}$ −65.9. These line intensities were obtained for a contact time of 10 ms, corresponding to an optimized value. An important experimental detail can be added: the Hartmann–Hahn condition was set up using compound **1**, maximizing the intensities of both lines. In addition, another test for the Hartmann–Hahn set-up was the resolution of both lines (with small intrinsic linewidths, ≈8–10 Hz), which was maximal at exact Hartmann–Hahn condition. In other words, compound **1** can be safely used as a standard for the set-up of CP experiments, a well resolved free induction decay (FID) being observed after eight scans (recycle delay = 15 s). At intermediate MAS rate (ν_{rot} = 1000 Hz, not shown here) two sets of spinning sidebands (with low intensities) were observed. Definitions of the shielding anisotropy (Δσ) and asymmetry (η) are given in Table 3. The anisotropy was estimated to be +35 ppm for both

Table 3 Silicon-29 and ^{13}C CP NMR data for compounds **1** and **2** and cadmium acetylacetonate including isotropic shielding (σ_{iso}), shielding-tensor components (σ_{ii}), shielding anisotropy ($\Delta\sigma$), asymmetry (η), linewidth, relative intensities and assignments [a]

Compound	σ_{iso}	σ_{33}	σ_{22}	σ_{11}	$\Delta\sigma$	δ_A	η	Linewidth/Hz	Relative intensity (%)	Assignment
1 (^{29}Si)	+80.4	+103.1	+68.9	+68.9	+34.2	+22.8	0.00	8	25	Si(1)
	+79.9	+102.7	+71.8	+65.1	+34.2	+22.8	0.30	10	75	Si(2)
(^{13}C)	−138.0	−216.6	−110.4	−92.0	−114.4	−74.3	0.20	18	13	C(11)
	−138.5	−214.6	−119.4	−81.9	−114.0	−75.9	0.50	18	32	C(21) [b]
	−128.8	−186.2	−116.0	−84.5	−85.9	−57.3	0.55	15	55	C(1)/C(2)
2 (^{13}C)	−135	−205	−118	−83	−105	−70	0.5	280	≈50	CH_2
	−129	−184	−124	−80	−83	−55	0.8	225	≈50	CH
[Cd(acac)$_2$] (^{13}C)	−102.1	−196.4	−55.1	−55.1	−141.3	−94.2	0.00	31	50	CH
	−100.6	−194.8	−53.5	−53.5	−141.3	−94.4	0.00	34	50	CH

[a] $\sigma = -\delta$ (in ppm); $\sigma_{iso} = \frac{1}{3}(\sigma_{11} + \sigma_{22} + \sigma_{33})$; $|\sigma_{33} - \sigma_{iso}| \geqslant |\sigma_{11} - \sigma_{iso}| \geqslant |\sigma_{22} - \sigma_{iso}|$; the errors in σ_{ii} values are typically ±2 ppm; $\Delta\sigma = \sigma_{33} - \frac{1}{2}(\sigma_{11} + \sigma_{22}) = \frac{3}{2}\delta_A$; $\delta_A = \sigma_{33} - \sigma_{iso}$; $\eta = (\sigma_{22} - \sigma_{11})/\delta_A$; typical error in η is ±0.1. [b] Corresponding to the average value of σ[C(21)]–σ[C(24)].

^{29}Si sites. In order to get an accurate determination of ($\Delta\sigma$, η) for each ^{29}Si site, an experiment at much lower MAS rate (ν_{rot} = 500 Hz) and at higher field [Ξ(^{29}Si) = 79.5 MHz] was used [Fig. 2(*b*)]. Assuming that the shielding is the only magnetic influence on the intensities of the spinning sidebands, both patterns were analysed by a standard graphical procedure [39,40] [Fig. 2(*d*)]. Sets of ($\Delta\sigma$, η) values were (+34.2 ppm, ≈0) for Si(1) and (+34.2 ppm, ≈0.2) for Si(2) leading to axial or nearly axial shielding tensors. However, the exact determination of η for axial or nearly axial symmetry using graphical methods is very difficult, whereas the shielding anisotropy is reasonably well defined.[41] Therefore, the static powder spectrum [Fig. 2(*c*)] was simulated with a unique set of parameters (η_1, η_2) and fixed anisotropy ($\Delta\sigma$ = +34.2 ppm) [Fig. 2(*e*)]. The best simulation was obtained with η_1 = 0.0 for Si(1) and η_2 = 0.3 for Si(2). The static pattern could not be described by two tensors having the same η parameter. The shielding tensor relative to Si(2) is non-axial whereas the Si(1) tensor can be considered as axial. However, the deviation from axiality for Si(2) remains rather low. The value of the anisotropy is in accord with values obtained for various organosilicon derivatives.[38]

The ^{13}C NMR spectrum of compound **1** is characterized by three isotropic resonances centred at δ 138.0, 138.5 and 128.8 [Fig. 3(*a*)]. The group of lines at δ 138.0/138.5 and the line at δ 128.8 are roughly in the ratio 1:1. The lines at δ 138.0 and 138.5 are roughly in the ratio 1:3. This intensity analysis was done for a contact time t_{CP} = 5 ms, corresponding to an optimized value. Indeed, all magnetizations reached their maximum for $t_{CP} \geqslant 5$ ms as shown by a variable-contact-time experiment [$T_{1\rho}$(^{1}H) ≈ 200 ms, *i.e.* $T_{1\rho}(^1H) \gg T_C$ and T_D, see below]. Both groups of lines are distinguished not only by isotropic chemical shifts but also by shielding anisotropies [Fig. 3(*b*), 3(*c*) and Table 3]. These observations indicate that each group of resonances may be assigned to CH or CH_2 sites (direct definite assignment is not straightforward at this stage). The sideband pattern corresponding to δ 128.8 [Fig. 3(*b*)] consists of narrow lines of equal width: this ascertains the set-up of the magic angle. It has been shown that off-axis sample spinning in the slow-spinning regime led to distorted sideband patterns and could result in misinterpretations of the spectra [42] (especially in the case of high ^{13}C shielding anisotropies). Therefore, the resonances closely centred at δ 138.0 and 138.5 do correspond to isotropic peaks and are not artifacts. In this sense compound **1** could be used as a secondary reference for precise magic angle set-up (at least on the ^{13}C chemical shift scale).

Shielding anisotropies ($\Delta\sigma$) for C(1)/C(2), C(11) and C(21) (see Table 3) are small when compared to common values observed for rigid entities $R^1R^2C{=}CR^3R^4$.[43,44] This may suggest motional averaging at the vinyl sites leading to a drastic reduction in CSA values for every ^{13}C site.[45] This point will be carefully analysed by using the IRCP technique. Such a NMR sequence will allow also definite assignments for the observed lines.

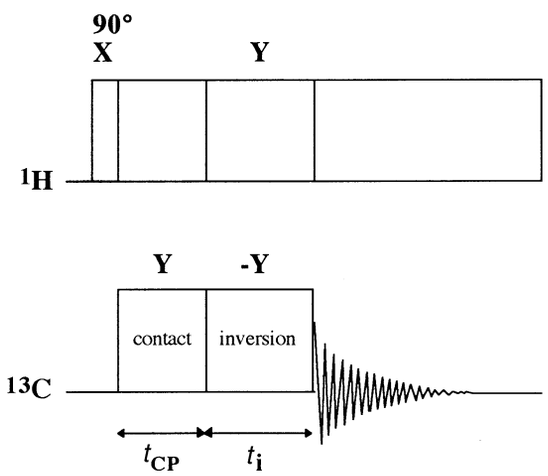

Fig. 4 An IRCP sequence based on a standard ^{13}C CP MAS experiment: [48] t_{CP} = contact time (fixed) and t_i = inversion time (variable)

Investigation by IRCP techniques. A few sequences based on CP NMR allow one to edit ^{13}C resonance lines in connection with the number of directly bonded protons. The most commonly used sequence is referred to in the literature as NQS (non-quaternary suppression). First introduced by Alla and Lippmaa [46] and developed by Opella and Frey,[47] it allows one to distinguish between rigid protonated groups (such as CH and CH_2) and weakly coupled sites (such as carbonyl or quaternary C) by dipolar dephasing. Methyl has an intermediate behaviour due to fast reorientation, leading to a substantial reduction in the dipolar coupling strength. However, this sequence fails to distingish between 'rigid' CH and CH_2 groups.[48] Indeed, CH and CH_2 have similar dipolar dephasing constants; moreover, these constants can largely be modulated by molecular motion. A second approach to spectral editing is related to solid-state J spectroscopy combined with multipulse on the ^{1}H channel.[49] However, so far, this has been applied mainly to species with high intrinsic mobilities and very rarely to rigid solid compounds. More recently, sequences based on polarization/inversion of polarization have been widely developed in the framework of spectral editing.[48,50]

The IRCP sequence used in this work is presented in Fig. 4. It is derived from a standard CP sequence: after a contact time t_{CP} (long enough to polarize all ^{13}C nuclei), a 180° phase shift is operated on the ^{13}C channel. Owing to spin–temperature inversion, the obtained carbon-13 magnetization will invert during the inversion time t_i. Then, the remaining ^{13}C signal is acquired, including high-power decoupling. This experiment is also called CPPI (cross polarization with polarization inversion).[48] It has been demonstrated that cross-polarization dynamics and polarization inversion dynamics are identical.[51] In the case of strongly coupled sites (such as CH and CH_2), analytical expres-

sions of the magnetizations during the inversion process have been derived for powdered samples at moderate MAS (≪10 kHz), neglecting relaxation,[48] equation (1) where M^0 represents

$$M(^{13}CH_n) = M^0\left[\frac{2}{n+1}\exp\left(-\frac{t_i}{T_D}\right) + \frac{2n}{n+1}\exp\left(-\frac{3}{2}\frac{t_i}{T_D}\right)\exp\left(-\frac{t_i^2}{T_C^2}\right) - 1\right] \quad (1)$$

the maximal magnetization reached after t_{CP} and n corresponds to the number of directly bonded protons in the CH_n group. The inversion of polarization is characterized by two time constants which are related to different types of magnetization transfer: T_C accounts for the coherent transfer of magnetization, involving the ^{13}C nucleus and the directly bonded protons; it can be considered as an inverse measure of the strength of the heteronuclear dipolar coupling for CH_n groups. It can be estimated for rigid CH_n groups. Rapid molecular motion will lead to a reduction in dipolar coupling and will be related therefore to an increase in T_C. Parameter T_D is related to spin-diffusion processes, which involve all the remaining protons. Equation (1) is a generalization of that first derived by Müller *et al.*,[52] accounting for magnetization oscillations in CP transfer for ferrocene single crystals. Generally, $T_C \ll T_D$ and the polarization inversion can be described by two regimes: the first (first tens of microseconds for t_i) is dominated by a rapid decay of $M(^{13}CH_n)$, characterized by T_C. Then, a much slower regime of inversion follows (T_D). As the dynamics of the two regimes are very different, a sharp turning point is observed. It corresponds to the end of the fast regime of inversion. Then, the magnetization reaches $(1 - n)(1 + n)^{-1}M^0$ [equation (1)]. The CH and CH_2 groups can be distinguished by the value of their turning point: 0 and $-\frac{1}{3}M^0$, respectively. In this sense spectral editing is achieved. Moreover, it has been demonstrated that the criterion of the turning point is much less sensitive to molecular motions than are methods which rely only on the relative strengths of dipolar couplings (NQS sequence). In the case of weakly coupled sites (such as C=O, quaternary C or rapidly rotating Me), the inversion of polarization is well described by an exponential process and one unique time constant, equation (2), again neglecting relaxation; T_{CH} is the

$$M(^{13}C) = M^0\left[2\exp\left(-\frac{t_i}{T_{CH}}\right) - 1\right] \quad (2)$$

standard cross-polarization constant. Equation (2) corresponds to the standard thermodynamic approach of cross-polarization dynamics.[28]

The IRCP sequence (^{13}C) has been applied to the study of compound **1** and to gel **2**. Our goal was to propose definite assignments for the ^{13}C lines and possibly to obtain information about molecular motions. Spectra obtained for compound **1** (rotation speed = 4 kHz) with different increments of t_i are presented in Fig. 5. At this rotation speed only two sets of spinning sidebands (with low intensities) are observed. The inversion of the normalized magnetization intensities is presented in Fig. 6. The total magnetization of the group of resonances centred at δ 138.0 and 138.5 was considered. The IRCP sequence was also applied to a sample of cadmium acetylacetonate [Cd(MeCOCHCOMe)$_2$], *i.e.* [Cd(acac)$_2$] (see Experimental section). In this compound the acetylacetonate ligands are stabilized in the enol form showing CH spin pairs with sp^2 carbon atoms. This metalloorganic compound can act as a reference for 'rigid' $C_{sp^2}H$ groups. Actually, two CH resonances are observed due to acetylacetonate moieties consistent with crystallographic data.[53] Shift parameters are presented in Table 3. It is clearly seen that both inversions for $\langle\delta\rangle \approx 138$ and δ 128.8 present two regimes: a rapid one during the first 100 μs and a much slower one for

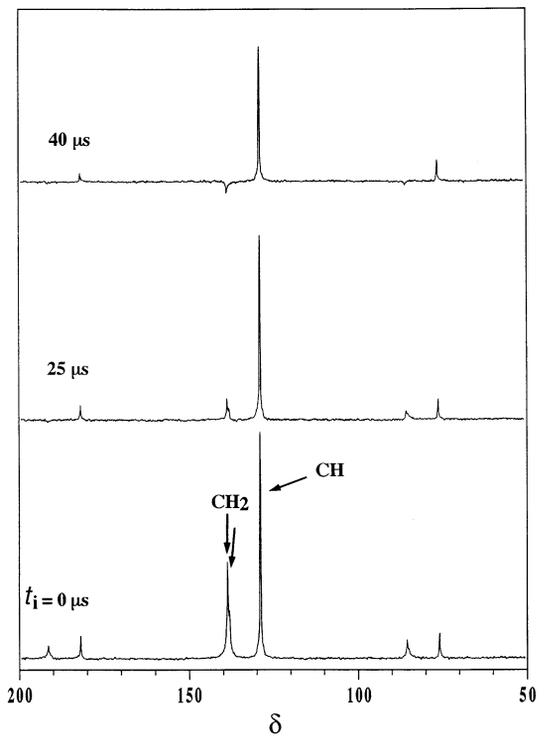

Fig. 5 The ^{13}C IRCP MAS NMR spectra of compound **1** (t_{CP} = 5 ms); t_i = 0 μs corresponds to a standard CP MAS experiment (ν_{rot} = 4000 Hz, N_s = 48, l.b. = 10)

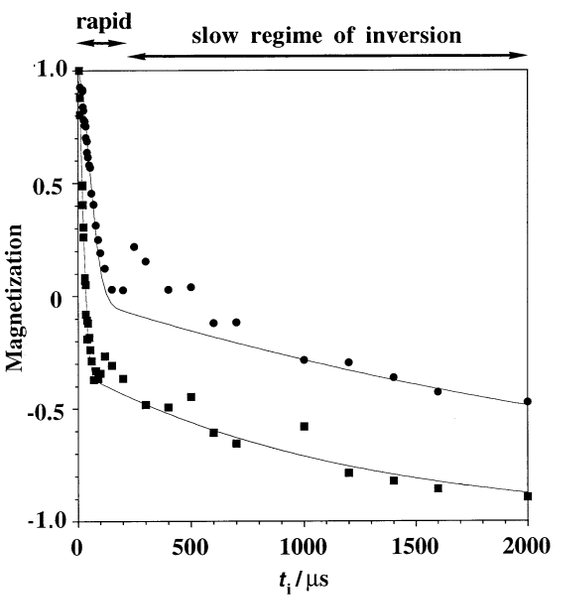

Fig. 6 Evolution of the magnetizations (compound **1**) *versus* inversion time t_i. Fits are related to equation (1) (with n = 1 for CH and n = 2 for CH_2). ●, δ 128.8; ■, $\langle\delta\rangle \approx 138$

higher values of t_i. However, the turning points between the two regimes are obviously different. For δ 128.8 it corresponds roughly to 0; for $\langle\delta\rangle \approx 138$ it corresponds roughly to $-\frac{1}{3}$. Inversion curves were fitted using equation (1). Best fits were obtained with n = 1 (δ 128.8) and 2 ($\langle\delta\rangle \approx 138$). Fits obtained with equation (2) involving a unique time constant were very poor. The extracted values of T_C and T_D are presented in Table 4. It is then possible to confirm assignments on the basis of the inversion curves. The resonance centred at δ 128.8 is assigned to CH groups (n = 1); both resonances at δ 138.0 and 138.5 are assigned to CH_2 groups (n = 2). As indicated above, it is also obvious that $T_D \gg T_C$. We should mention at this stage that the resonance at δ 128.8 and its spinning sidebands are flanked by

Table 4 Extracted T_C and T_D values from ^{13}C IRCP MAS NMR experiments according to equation (1)

Compound	^{13}C site	T_C/μs	T_D/ms
1	CH[C(1)/C(2)]	75 ± 4	3 ± 0.7
	CH_2[C(11)/C(21)]	30 ± 2	1.3 ± 0.2
2	CH	80*	3.5*
	CH_2	30 ± 2	2.2 ± 0.3
[Cd(acac)$_2$]	CH	25 ± 0.6	0.43 ± 0.02

* Estimation, see text.

two satellites [see the insert in Fig. 3(*a*)]. The satellites are assigned to ^{13}C nuclei coupled to ^{29}Si [natural abundance 4.7% and $|^1J(^{13}C–^{29}Si)| = 136 \pm 5$ Hz]. The ^{13}C INEPT study (see Experimental section) of the molecular precursor $Si(C_2H_3)(OEt)_3$ confirmed these results: (*i*) the CH_2 signal was less shielded than the CH signal, (*ii*) $|^1J(^{13}C–^{29}Si)| = 119$ Hz, in agreement with the value observed in the solid state. The signal centred at δ 128.8 corresponds obviously to C(1) and C(2) resonances (see crystallographic section above). These resonances are not resolved as the isotropic chemical shifts must be very similar. The extracted value of T_C for CH_2 (Table 4) is clearly higher than those observed for 'rigid' aliphatic CH_2 groups.[48,54] Moreover, the magnetization related to CH_2 in compound **1** is still positive for $t_i = 25$ μs (Fig. 5), whereas the magnetization of CH_2 in glycine ($NH_2CH_2CO_2H$) is slightly negative for the same inversion time (see Experimental section). Owing to slightly shorter C–H bond lengths, a 'rigid' $C_{sp^2}H_2$ group should invert more rapidly than a 'rigid' aliphatic $C_{sp^3}H_2$ group. For compound **1** such experimental observations suggest motional reduction of the dipolar coupling between ^{13}C and the directly bonded protons. As the dipolar constant T_C is significantly affected, the frequency of the motion can be estimated to be $\nu \geqslant 10^5$ Hz.[55] At this stage we can conclude that the apparent disorder observed for C(11) and C(21) by X-ray diffraction cannot be related to a static one. Indeed, in this case the behaviour of the rigid CH_2 groups should be characterized by $T_C(CH_2) < T_C(CH)$ for [Cd(acac)$_2$], which is obviously not the case (Table 4).

Fast anisotropic motion of the vinyl groups (considered as rigid entities) around the Si(1)–C(1) and Si(2)–C(2) bonds may then be considered. The crystallographic refinements show that the local motion of the vinyl groups may consist of rapid jumps between discrete positions: three symmetry-related positions for C(11) and (at least) four for C(21). It is known that a continuous rotation of vinyl groups is not necessary to obtain averaging of dipolar coupling under reorientation. Rapid jumps between p positions ($p \geqslant 3$) located on a regular polygon lead exactly to the same averaging. By symmetry, the three C(11) positions (with equal occupancy) describe an equilateral triangle. The four C(21) positions describe a distorted square but refinement in this case is much less safe. If the approach of rapid motion of the vinyl groups is correct two points remain open: (*i*) T_C for CH is much higher than T_C observed for CH_2 in compound **1** (see Table 4), which indicates a much stronger reduction of the dipolar coupling in the case of the CH spin pair; (*ii*) the fits of the IRCP curves (Fig. 6) obtained with equation (1) are less reliable for higher values of t_i. Let us answer these two questions, considering reorientation of the vinyl groups around the Si–C bonds.

(*i*) The approximate geometry of one vinyl group is represented in Fig. 7. Angles β_i ($i = 1$–3) are those related to the atoms Si(1), C(1), C(11), H(1), H(2) and H(3) (see Fig. 1). Let us first consider the strong dipolar coupling between the CH spin pair. In a static configuration the dipolar tensor corresponding to CH is axially symmetric with the C–H bond direction as a unique axis. If we consider rapid anisotropic reorientation around the Si–C direction (rapid jumps) the dipolar tensor remains axially symmetric but with the Si–C bond as a new

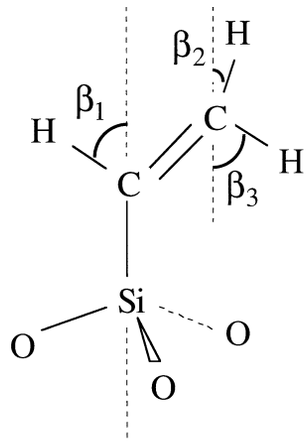

Fig. 7 Approximate geometry of the vinyl group corresponding to atoms Si(1), C(1) and C(11) and to related H atoms (*calculated* positions): $\beta_1 \approx 63$, $\beta_2 \approx 6$ and $\beta_3 \approx 54°$

unique axis. Then, the dipolar coupling 'strength' is modulated by the factor $R = (3\cos^2\beta - 1)/2$, where β corresponds to the angle between the C–H bond and the axis of rotation. This result is general[45] and can be transposed for any second-rank tensor such as CSA and J coupling (when considering first-order effects on the lineshapes). When the tensor is not axially symmetric the reduction factor for the interaction is a more complex function of the principal values of the tensor and the Euler angles between the principal axes and the reorientation direction. In the case of CH, $\beta_1 \approx 63°$ so that $|R| \approx 0.2$. In other words, this particular geometry of the CH pair leads to a very strong reduction in dipolar coupling under rapid reorientation. This can explain the high value of T_C observed for the CH group in the IRCP experiment. The IRCP curves of [Cd(acac)$_2$] (containing 'rigid' CH groups), compound **1** and ferrocene [Fe(η-C_5H_5)$_2$] (adapted from ref. 56 and neglecting rotational echoes, see below) are presented in Fig. 8. We assume for this comparison that the C–H bond lengths are nearly equal for the three compounds. The rigid CH in [Cd(acac)$_2$] experiences strong dipolar coupling leading to a low value of T_C and rapid inversion during the first tens of μs. Ferrocene is characterized by rapid rotation around the internal axis with $\beta = 90°$ ($|R| = 0.5$);[56] its evolution is intermediate between the rigid case of [Cd(acac)$_2$] and the behaviour of the vinyl groups in compound **1** as expected from inspection of the R values. In the case of methylene groups (CH_2), $\beta_2 \approx 6$ and $\beta_3 \approx 54°$. This means that the C–H(2) bond is nearly collinear with the rotation axis whereas the C–H(3) bond is nearly at the magic angle. The C–H(2) dipolar coupling 'strength' is therefore almost unaffected by the motion ($R \approx 1$). The removal of dipolar coupling from H(3) is almost complete. Therefore, the inversion of the CH_2 magnetization is rapid during the first tens of microseconds ($T_C = 30$ μs) but less than for a 'rigid' CH_2 group. This T_C value is comparable to values observed for rigid CH groups. We have shown that simple geometrical arguments may explain the different evolutions of CH and CH_2 magnetizations. These results are at best qualitative since β_i angles are estimated through the calculated positions of the H atoms. Conversely, theoretical analysis of the IRCP curves may lead to the determination of particular angles and bond lengths in the molecule.

(*ii*) In the case of ferrocene the second stage of polarization inversion was modulated by strong rotational echoes.[56] Indeed, the interactions between CH pairs are periodically refocused by MAS at times $t_n = (n2\pi/\omega_{rot}) = (n/\nu_{rot})$ with $n = 1$, 2 *etc.*, ν_{rot} being the spinning frequency. In our experiments, $\nu_{rot} = 4000$ Hz and $t_1 = 250$ μs, $t_2 = 500$ μs, *etc.* Such echoes could explain the fact that the calculated curves in Fig. 6 are less reliable in the second stage of polarization inversion. Nevertheless, the order of magnitude for extracted T_D values is correct.

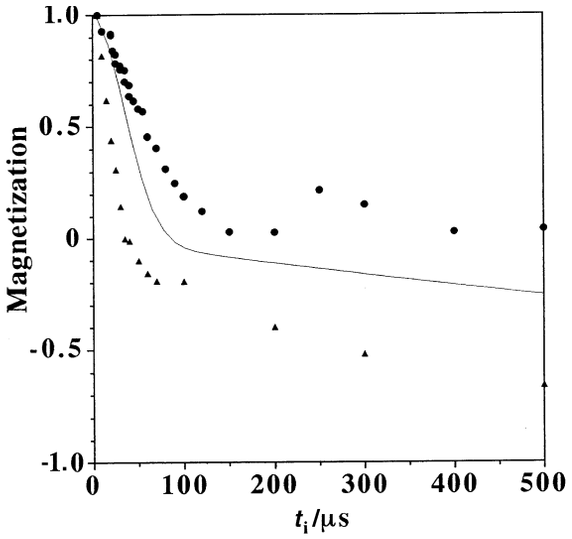

Fig. 8 Evolution of $C_{sp^2}H$ magnetization *versus* inversion time t_i (IRCP sequence) for: ▲, cadmium acetyloacetonate ('rigid' CH); ——, ferrocene, adapted from ref. 56 with $T_C = 50$ μs and $T_D = 1.7$ ms, $|R| = 0.5$; ●, compound **1** (expansion of Fig. 6), $|R| \approx 0.2$

The ^{13}C CSA should also be modulated by vinyl reorientations. As stated above, CSA values for all carbon-13 sites are unusually small. However, the interpretation for the reduction of $\Delta\sigma$ is difficult. The CSA can be represented by a second-rank tensor, characterized by three initial principal values. Upon rapid reorientation, the reduction in CSA can be represented by a new tensor which is axially symmetric. The new principal values are functions of the initial values and Euler angles between the reorientation axis and the initial principal axes.[45] In the case of compound **1** the orientations of the different CSA principal axes systems in the 'static' configuration of the cubane are not known. In other words, the Euler angles which orientate the initial tensor from the Si–C bond are not known. The IRCP results, concerning the reduction of dipolar tensors, are easier to analyse than the $\Delta\sigma$ reduction, as the CH direction corresponds to a principal direction of the initial dipolar tensor. Therefore, the IRCP results and $\Delta\sigma$ reduction cannot be directly related.

As a conclusion the IRCP dynamics study allows a deep insight into the dipolar local fields. The ^{13}C spectra can be edited completely (CH and CH_2 distinction) though strong reduction of the dipolar coupling was present. Turning points in the IRCP curves are safe criteria for spectral editing. Reorientation of the vinyl groups could explain the different magnetization behaviours during the IRCP sequence. Moreover, the reorientation of the vinyl groups could be considered independently from the cubane core of the molecule as will be seen below. Finally, one should note that such different CP dynamics for closely spaced CH and CH_2 may have a considerable influence on quantification by ^{13}C CP MAS NMR spectroscopy and may lead to misinterpretations in spectral editing. One must be aware of specific molecular motions leading to strongly reduced dipolar coupling.

Compound 2 (xerogel). *Standard* ^{29}Si *and* ^{13}C *CP MAS experiments.* The ^{29}Si CP MAS spectrum (not shown) of compound **2** is characterized by a major peak centred at δ −78 (linewidth ≈ 350 Hz), which corresponds to fully condensed T^3 units $C_2H_3Si^*(OSi\equiv)_3$. A minor peak centred at δ −72 is also observed and corresponds to T^2 units $C_2H_3Si^*X(OSi\equiv)_2$ with X = OH or OEt. This demonstrates that the network of silicon entities is highly condensed. Spectra of compound **2** obtained by ^{13}C CP MAS are presented in Fig. 9 ($t_i = 0$ μs) and NMR data corresponding to the ^{13}C vinyl resonances are presented in Table 3. The CP spectrum has two peaks located at δ 135 and 129 and two minor resonances assigned to residual ethoxy groups (δ 58 and 17: CH_2 and CH_3, respectively). Low-speed sideband patterns related to vinylic ^{13}C can be well simulated by two sets of average ($\Delta\sigma$, η) CSA values (see Table 3 and Fig. 10). The $\Delta\sigma$ values are in agreement with those observed for compound **1**, suggesting again rapid reorientation of vinyl groups around Si–C bonds.

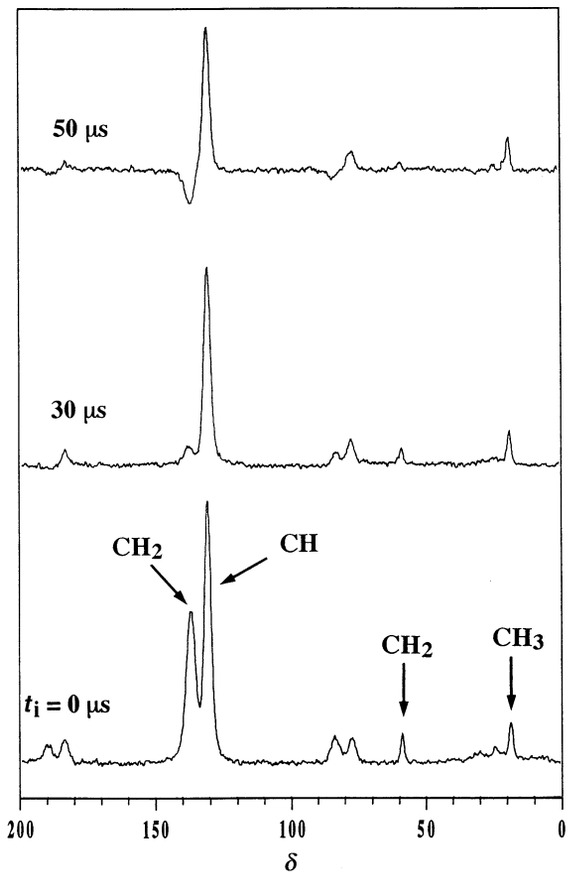

Fig. 9 The ^{13}C CP and IRCP MAS NMR spectra of compound **2**: $\nu_{rot} = 4000$ Hz, Ξ (^{13}C) = 75.46 MHz, φ = 4 mm, $N_s = 600$, $t_{CP} = 5$ ms, r.d. = 6 s, l.b. = 30 Hz

Investigation by ^{13}C *IRCP MAS NMR.* The IRCP spectra obtained for $t_i = 30$ and 50 μs are presented in Fig. 9. Evolution of both magnetizations (vinylic CH and CH_2) is presented in Fig. 11. Simulations were obtained using two peaks with fixed isotropic chemical shift and linewidth. Only amplitudes were allowed to vary. The inversion of magnetization shows clearly two regimes for both resonances and equation (1) was used to extract T_C and T_D values. Once again, spectral editing is easy and the less shielded peak (δ 135) can be safely assigned to CH_2 [$n = 2$ in equation (1)]. The fit obtained for δ 129 (using $n = 1$) is less safe because the turning point between the two regimes of inversion is higher than 0; T_C and T_D values are given as estimations. However, the CH IRCP behaviours for compounds **1** and **2** are identical during the first tens of μs. The T_C values are in very close agreement with those extracted for CH and CH_2 in compound **1**. This indicates that the motion of the vinyl groups localized around Si–C bonds is independent of the rest of the structure (*i.e.* the cubane cage in the case of compound **1**). The T_D values are of the same order of magnitude but show some variations between compounds **1** and **2**. This is not surprising as T_D is strongly influenced by the ^1H–^1H interactions, which may vary considerably from one compound to another.

Conclusion

Octameric vinylsilasesquioxane **1** has been studied by X-ray diffraction and $^{29}Si/^{13}C$ CP MAS NMR spectroscopy. The X-ray data showed an uncertainty about the vinyl CH_2 positions

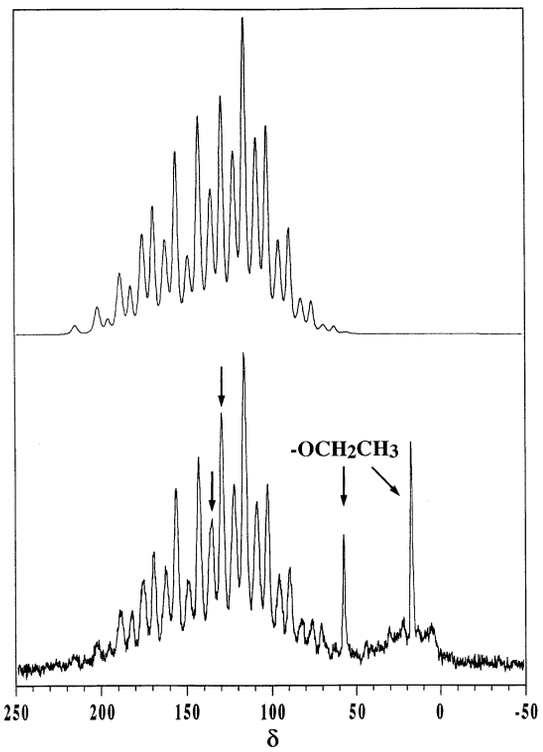

Fig. 10 Low-rotation-speed ^{13}C CP MAS spectrum (lower) of compound **2**. Only the vinyl CH and CH_2 patterns are simulated (upper): ν_{rot} = 1000 Hz, Ξ (^{13}C) = 75.46 MHz, φ = 7 mm, N_s = 1688, t_{CP} = 5 ms, r.d. = 6 s, l.b. = 10 Hz. Isotropic resonances are labelled by arrows

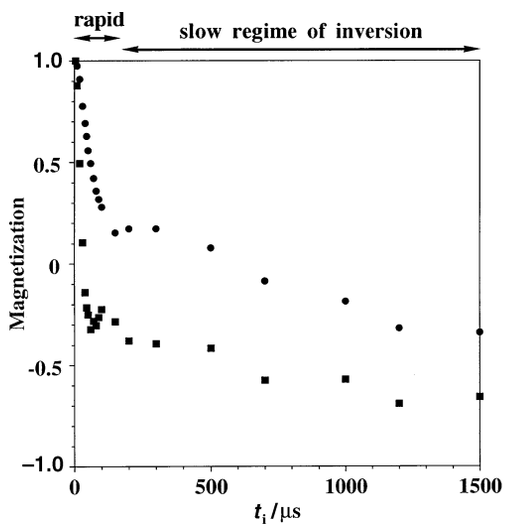

Fig. 11 Evolution of the magnetizations (compound **2**) *versus* inversion time t_i for vinylic CH and CH_2 signals: ●, δ 129; ■, δ 135

owing to static disorder or rapid reorientation by jumping. The latter is in accord with a careful analysis of CP dynamics, which revealed the rapid anisotropic reorientation of the vinyl groups around the Si–C bonds. The frequency of the motion was certainly higher than 10^5 Hz, leading to a strong reduction in dipolar coupling. Adjacent CH and CH_2 groups showed very different residual dipolar coupling, as shown by IRCP. These observations were explained by the simple geometrical characteristics of the vinyl groups: the angle between the C–H and the Si–C bond axis was nearly the magic angle, leading to a very strong reduction in the dipolar coupling. Nevertheless, the CH polarization inversion showed two regimes as expected, allowing a complete spectral editing and definite assignments. The IRCP sequence can be safely used in solid-state NMR spectroscopy for the determination of proton multiplicities and can be compared to the liquid-state NMR sequences DEPT and INEPT. The high resolution of the spectra of **1** allows one to use this compound as a safe secondary reference for the set-up of ^{29}Si and ^{13}C CP NMR experiments.

The amorphous gel **2** was also studied by $^{29}Si/^{13}C$ CP NMR spectroscopy. It is a good example for applying NMR analysis techniques, which were carefully set with well defined compounds (such as crystals) to amorphous derived materials. The IRCP experiment also showed a strong reduction in dipolar coupling through motional averaging. Therefore, extreme caution should be taken when considering quantitative CP experiments. This could be especially important in the study of amorphous materials (bridged organofunctional silasesquioxanes, for instance), for which ^{13}C CP NMR spectroscopy is used in the quantification of bridging reactions between the different cubane cores.

Experimental

Syntheses

Compound 1 and derived gel 2. Triethoxyvinylsilane (Fluka) was used as received. The purity of this monomeric compound was checked by standard ^{13}C and ^{29}Si liquid-state NMR spectroscopy and INEPT[29] [relative to $SiMe_4$: δ_{Si} −58.7; δ_C(=CH) 130.5; δ_C(=CH_2) 135.8; δ_C(CH_2) 58.3; δ_C(CH_3) 18.3; $|^1J(^{13}C–^{29}Si)|$ = 119 Hz as shown by ^{13}C INEPT]. Acidic water (HCl, 0.1 mol l^{-1}) (0.35 g, 19.7 mmol) was added to $Si(C_2H_3)(OEt)_3$ (2.50 g, 13.1 mmol) with vigorous stirring, without any solvent (H_2O:Si = 1.5:1). After 2–3 min the mixture became homogeneous. At room temperature and after several days, single crystals of compound **1** were obtained as transparent parallelepipeds. These were extracted and washed with dried ethanol. They were insensitive to air moisture and found suitable for structure determination. Upon ageing the remaining liquid mixture led to a transparent gel which could be heated at 80 °C, leading to a dry amorphous powder called xerogel (compound **2**). Such powders were studied without further treatment. The yield of the crystallized phase was estimated to be a few %. Several single crystals were analysed by X-ray diffraction, leading to one unique crystallographic structure, corresponding to compound **1**. The IR spectrum was recorded and acted as 'fingerprint' of **1**. Many experiments were repeated to obtain crystals, the molecular structure of which was systematically checked by IR spectroscopy.

Cadmium acetylacetonate. Acetylacetone (pentane-2,4-dione, Fluka) (1 cm^3, 9.68 mmol) was slowly added at room temperature and with stirring to an alkaline aqueous solution of cadmium chloride (6 cm^3 of KOH solution at pH 14 + 20 cm^3 of $CdCl_2$ solution, $[Cd^{2+}]$ = 0.25 mol l^{-1}). The white precipitate immediately obtained was filtered off and washed with iced water. Crystalline cadmium acetylacetonate was identified by X-ray diffraction: according to the crystallographic data given in ref. 53, a powder diffractogram was simulated using FULLPROF program.[57] The experimental diffractogram and the simulation were strictly identical. Solid-state ^{13}C CP MAS NMR (contact time = 2 ms, recycle delay = 6 s, number of scans = 856): δ_C(C=O) 199.2, 193.8, 189.8 and 187.1; δ_C(=CH) 102.1 and 100.6; δ_C(CH_3) 30.2, 29.7 and 29.3. These isotropic chemical shifts are in very good agreement with those observed by Takegoshi *et al.*[58]

Spectroscopy

Infrared spectra were recorded at room temperature as pressed KBr pellets with a Nicolet Fourier-transform spectrometer (range 400–4000 cm^{-1}); liquid ^{13}C and ^{29}Si NMR spectra at room temperature on Bruker AC-300 (^{13}C, 75.46 MHz) and MSL-400 (^{29}Si, 79.50 MHz) spectrometers, respectively, using a Bruker VSP probe. Chemical shifts are referenced to $SiMe_4$. The ^{13}C INEPT sequence[29] (including decoupling from ^1H and refocusing) was also used to ascertain assignments (see Results

and Discussion). Solid-state ^{13}C and ^{29}Si CP MAS experiments were carried out using Bruker MSL-300 and MSL 400 spectrometers (^{13}C, 75.46; ^{29}Si, 59.62 and 79.50 MHz) equipped with Bruker probes including external lock (4 and 7 mm probes). Zirconia rotors were used. Solid samples were spun at 0.5–4 kHz. Fluctuations in MAS speed were smaller than ±2 Hz over several hours. The magic angle was carefully set using the ^{79}Br resonance of KBr. The matching condition for the Hartmann–Hahn cross-polarization (^{1}H 90° pulse length: 5 μs for the 4 mm probe and 6.5 μs for the 7 mm probe) was set on adamantane (^{13}C) and compound **1** (^{29}Si). It should be noted that both radio-frequency channel levels have to be very carefully set. Indeed, it has been demonstrated that under mismatched conditions the results of IRCP sequences may be false.[48] In order to check the matching of the Hartmann–Hahn condition, the IRCP seqence was tested on a glycine sample which acts as a typical 'rigid' methylene CH_2 group (see Results and Discussion). The test was done periodically during all ^{13}C IRCP MAS experiments. Contact times (t_{CP}) were optimized by standard variable-contact-time experiments. Relaxation delays were 6–15 s. The ^{13}C and ^{29}Si shielding-tensor analyses,[39] as well as deconvolution of lines, were obtained by using the WINFIT program developed by Massiot *et al.*[40]

Crystallography

Crystals of compound **1** were prepared as described above, sealed in Lindemann capillaries and studied at 293 K.

Crystal data. $C_{16}H_{24}O_{12}Si_8$, $M = 633.04$, trigonal, space group $R\bar{3}$ (no. 148), $a = 13.533(2)$, $c = 14.222(2)$ Å, $\gamma = 120°$, $U = 1012(5)$ Å^3 (by least-squares refinement for 25 reflections in the range $13.9 < \theta < 14.5°$, $\lambda = 0.710\ 69$ Å), $Z = 3$, $D_c = 1.398$ g cm^{-3}, $F(000) = 984$. Colourless parallelepipeds. Crystal dimensions 0.4 × 0.3 × 0.3 mm, μ(Mo-Kα) = 0.4 mm^{-1}.

Data collection. Enraf-Nonius CAD-4 diffractometer, ω–2θ mode with ω scan width = 0.80 + 0.34 tan θ, ω-scan speed 2–20.1 min^{-1}, graphite-monochromated Mo-Kα radiation, 999 reflections measured ($1 \leqslant \theta \leqslant 25°$; h 0–13, k 0–13; l −16 to 16), 882 independent, giving 332 with $I \geqslant 3\sigma(I)$ (merging R = 0.0166). Two standard reflections were used (intervals: 100 reflections and 60 min). Variation of standards: 1%.

Structure solution and refinement. Direct methods (Si, O, C), full-matrix least-square refinements with anisotropic thermal parameters in the last cycles for all non-H atoms and hydrogens in calculated positions (assuming sp^2 C atoms). Occupancies of C(11), C(21)–C(24) positions were also refined. As μ(Mo-Kα) was rather low, no absorption correction was applied. Sixty-eight refined parameters. Extinction correction method:[59] secondary extinction 36(9). The weighting scheme was $w = 1$. Final R and R' values were 0.0503 and 0.0480; $(\Delta/\sigma)_{max} = 0.15$. A final Fourier-difference calculation showed residual electron density in the range −0.2 to +0.15 e Å^{-3}. The SHELXS 86[60] system of computer programs was used for the direct methods. Refinement was performed with the CRYSTALS program.[61] Atomic scattering factors, corrected for anomalous dispersion, were obtained from ref. 62.

Atomic coordinates, thermal parameters, and bond lengths and angles have been deposited at the Cambridge Crystallographic Data Centre (CCDC). See Instructions for Authors, *J. Chem. Soc., Dalton Trans.*, 1997, Issue 1. Any request to the CCDC for this material should quote the full literature citation and the reference number 186/438.

Acknowledgements

We thank Professor P. Boch for his support and Professor R. M. Laine for providing different octameric silasesquioxanes. S. Mace is also gratefully acknowledged for experimental help.

References

1 M. G. Voronkov and V. I. Lavrent′yev, *Top. Curr. Chem.*, 1982, **102**, 199.
2 F. J. Feher and T. A. Budzichowski, *Polyhedron*, 1995, **22**, 3239.
3 R. H. Baney, M. Itoh, A. Sakakibara and T. Suzuki, *Chem. Rev.*, 1995, **95**, 1409.
4 D. A. Loy and K. J. Shea, *Chem. Rev.*, 1995, **95**, 1431.
5 C. L. Frye and W. T. Collins, *J. Am. Chem. Soc.*, 1970, **92**, 5586.
6 P. A. Agaskar and W. G. Klemperer, *Inorg. Chim. Acta*, 1995, **229**, 355 and refs. therein.
7 F. J. Feher, T. A. Budzichowski and K. J. Weller, *J. Am. Chem. Soc.*, 1989, **111**, 7288.
8 F. J. Feher and K. J. Weller, *Organometallics*, 1990, **9**, 2638.
9 K. Larsson, *Ark. Kemi*, 1960, **16**, 203, 209, 215.
10 I. A. Baidina, N. V. Podberezskaya, V. I. Alekseev, T. N. Martynova, S. V. Borisov and A. N. Kanev, *Zh. Strukt. Khim.*, 1979, **20**, 648; N. V. Podberezskaya, S. A. Magarill, I. A. Baidina, S. V. Borisov, L. E. Gorsh, A. N. Kanev and T. N. Martynova, *J. Struct. Chem.* (*Engl. Transl.*), 1982, **23**, 422.
11 G. Koellner and U. Müller, *Acta Crystallogr., Sect. C*, 1989, **45**, 1106.
12 F. J. Feher and T. A. Budzichowski, *J. Organomet. Chem.*, 1989, **373**, 153.
13 H. B. Bürgi, K. W. Törnroos, G. Calzaferri and H. Bürgy, *Inorg. Chem.*, 1993, **32**, 4914.
14 G. Calzaferri, R. Imhof and K. W. Törnroos, *J. Chem. Soc., Dalton Trans.*, 1994, 3123.
15 K. W. Törnroos, H. B. Bürgi, G. Calzaferri and H. Bürgy, *Acta Crystallogr., Sect. B*, 1995, **51**, 155.
16 K. W. Törnroos, G. Calzaferri and R. Imhof, *Acta Crystallogr., Sect. C*, 1995, **51**, 1732.
17 K. W. Törnroos, *Acta Crystallogr., Sect. C*, 1994, **50**, 1646.
18 M. Bärtsch, P. Bornhauser, G. Calzaferri and R. Imhof, *J. Phys. Chem.*, 1994, **98**, 2817.
19 B. J. Hendan and H. C. Marsmann, *J. Organomet. Chem.*, 1994, **483**, 33.
20 J. Kowalewski, T. Nilsson and K. W. Törnroos, *J. Chem. Soc., Dalton Trans.*, 1996, 1597.
21 E. Lippmaa, M. A. Alla, T. J. Pehk and G. Engelhardt, *J. Am. Chem. Soc.*, 1978, **100**, 1929.
22 G. Engelhardt, D. Zeigan, D. Hoebbel, A. Samoson and E. Lippmaa, *Z. Chem.*, 1982, **22**, 314.
23 J. D. Lichtenhan, Y. A. Otonari and M. J. Carr, *Macromolecules*, 1995, **28**, 8435.
24 S. E. Yuchs and K. A. Carrado, *Inorg. Chem.*, 1996, **35**, 261.
25 A. Sellinger and R. M. Laine, *Macromolecules*, 1996, **29**, 2327.
26 T. N. Martynova and V. P. Korchkov, *J. Organomet. Chem.*, 1983, **248**, 241.
27 T. N. Martynova and T. I. Chupakhina, *J. Organomet. Chem.*, 1988, **345**, 11.
28 A. Pines, M. G. Gibby and J. S. Waugh, *J. Chem. Phys.*, 1973, **59**, 569.
29 A. E. Derome, *Modern NMR Techniques for Chemistry Research*, Pergamon, Oxford, 1991, p. 129.
30 C. J. Brinker and G. W. Scherer, *Sol-Gel Science: The Physics and Chemistry of Sol-Gel Processing*, Academic Press, San Diego, 1990.
31 W. R. Schmidt, L. V. Interrante, R. H. Doremus, T. K. Trout, P. S. Marchetti and G. E. Maciel, *Chem. Mater.*, 1991, **3**, 257.
32 C. A. Fyfe and J. Niu, *Macromolecules*, 1995, **28**, 3894.
33 C. K. Johnson, ORTEP, Report ORNL-3794, Oak Ridge National Laboratory, Oak Ridge, TN, 1965.
34 G. Socrates, *Infrared Characteristic Group Frequencies*, Wiley, Chichester, 1994, p. 42.
35 D. Hoebbel, I. Pitsch, D. Heidemann, H. Jancke and W. Hiller, *Z. Anorg. Allg. Chem.*, 1990, **583**, 133.
36 I. Pitsch, D. Hoebbel, H. Jancke and W. Hiller, *Z. Anorg. Allg. Chem.*, 1991, **596**, 63.
37 A. R. Grimmer, R. Peter, E. Fechner and G. Molgedey, *Chem. Phys. Lett.*, 1981, **77**, 331.
38 R. K. Harris, T. N. Pritchard and E. G. Smith, *J. Chem. Soc., Faraday Trans. 1*, 1989, **85**, 1853.
39 J. Herzfeld and A. E. Berger, *J. Chem. Phys.*, 1980, **73**, 6021.
40 D. Massiot, H. Thiele and A. Germanus, *Bruker Rep.*, 1994, **140**, 43.
41 N. J. Clayden, C. M. Dobson, L. Y. Lian and D. J. Smith, *J. Magn. Reson.*, 1986, **69**, 476.
42 E. M. Menger, D. P. Raleigh and R. G. Griffin, *J. Magn. Reson.*, 1985, **63**, 579.
43 T. M. Duncan, *A Compilation of Chemical Shift Anisotropies*, The Farragut Press, Chicago, 1990, p. C-13.

44 A. M. Orendt, J. C. Facelli, A. J. Beeler, K. Reuter, W. J. Horton, P. W. Cutts, D. M. Grant and J. Michl, *J. Am. Chem. Soc.*, 1988, **110**, 3386.
45 M. Mehring, *Principles of High Resolution NMR in Solids*, Springer, Berlin, 1983, p. 50.
46 M. Alla and E. Lippmaa, *Chem. Phys. Lett.*, 1976, **37**, 260.
47 S. J. Opella and M. H. Frey, *J. Am. Chem. Soc.*, 1979, **101**, 5854.
48 X. Wu and K. W. Zilm, *J. Magn. Reson.*, 1993, **A102**, 205.
49 T. Terao, H. Miura and A. Saika, *J. Am. Chem. Soc.*, 1982, **104**, 5228.
50 X. Wu, S. T. Burns and K. W. Zilm, *J. Magn. Reson.*, 1994, **A111**, 29.
51 X. Wu, S. Zhang and X. Wu, *Phys. Rev. B*, 1988, **37**, 9827.
52 L. Müller, A. Kumar, T. Baumann and R. R. Ernst, *Phys. Rev. Lett.*, 1974, **32**, 1402.
53 E. N. Maslen, T. M. Greaney, C. L. Raston and A. H. White, *J. Chem. Soc., Dalton Trans.*, 1975, 400.
54 C. Bonhomme, J. Maquet, J. Livage and G. Mariotto, *Inorg. Chim. Acta*, 1995, **230**, 85.
55 F. Lauprêtre, L. Monnerie and J. Virlet, *Macromolecules*, 1984, **17**, 1397.
56 J. Hirschinger and M. Hervé, *Solid State NMR*, 1994, **3**, 121.
57 J. Rodrigues-Carvajal, FULLPROF 93, An Advanced Rietveld Code, Institut Laue-Langevin, Grenoble, 1993.
58 K. Takegoshi, K. J. Schenk and C. A. McDowell, *Inorg. Chem.*, 1987, **26**, 2552.
59 A. C. Larson, *Crystallographic Computing*, eds. F. R. Ahmed, J. R. Hall and C. P. Huber, Munksgaard, Copenhagen, 1970, p. 291.
60 G. M. Sheldrick, SHELXS 86, Program for the Solution of Crystal Structures, University of Göttingen, 1986.
61 D. J. Watkin, J. R. Carruthers and P. W. Betteridge, CRYSTALS, An Advanced Crystallographic Program System, Chemical Crystallography Laboratory, University of Oxford, 1988.
62 *International Tables for X-Ray Crystallography*, Kynoch Press, Birmingham, 1974, vol. 4.

Received 29*th January* 1997; *Paper* 7/00700K